Building a Sensorimotor Representation
of a Naive Agent's Tactile Space

Valentin Marcel, Sylvain Argentieri and Bruno Gas

Abstract—A new approach for robotics perception, rooted in the sensorimotor paradigm, is proposed in this paper. Making systems able to autonomously adapt themselves to changes in their own body or in their environment is still a challenging question for many different scientific communities. Multiple works propose either sophisticated adaptive model-based or learning-based techniques as a solution. Recent contributions have shown that it is possible for an agent to discover the structure of its interaction with the environment or its own body via the so-called sensorimotor flow. The presented work is based on this idea, and a method for building an internal representation of sensorimotor interaction is proposed, which does not require any *a priori* knowledge or model. A careful mathematical formalization is outlined, together with simulations, demonstrating the effectiveness of the approach. Several cases are considered allowing for a general discussion. Moreover, plausibility of the internal sensorimotor representation is highlighted by showing that it is possible to consider motion planning directly from it.

Index Terms—Active exploration of environment, robots with development and learning skills, using robots to study development and learning, applications.

I. INTRODUCTION

MORE and more researchers from different scientific fields (psychophysics, artificial intelligence, philosophy, ...) raise the question of how can a mobile agent perceive its environment without any model either of its environment or of itself. Of course, using *a priori* models of the environment can make robotic systems fast, efficient and robust when executing complex predefined tasks. But at the same time, such systems may have difficulties behaving autonomously, namely adapting themselves to unknown environments that have not been modeled or learned before –except by considering that a universal model could be obtained from a learning procedure.

A different path is proposed here, paved by Poincaré more than 100 years ago [1], [2]. In this line of research, what is called *perception* is not an innate capacity. It is something that is learned and can not be separated from motor action. Indeed, this *sensorimotor* flow carries fundamental information about the *external space* and its geometry [3]. For instance, Poincaré states that the external space dimension can be extracted from it by an agent endowed with several motor degrees of freedom and sensors whose outputs depend on the 3D position of the system. More generally, the sensorimotor flow indeed reveals some correlations, i.e. *sensorimotor contingencies* [4], which are invariant and carry information about the external

V. Marcel, S. Argentieri and B. Gas are with Sorbonne Universités, UPMC Univ. Paris 06, UMR 7222, ISIR, F-75005 Paris, France and CNRS, UMR 7222, ISIR, F-75005 Paris, France

environment of the agent. Philipona et al. proposed a mathematical formulation of this idea, not by using proprioceptive signals as suggested by Poincaré, but by exploiting sensor outputs signals instead [5]. The demonstration is based on the study of the sensory manifold and on its dimension. On this basis, the authors have been able to prove Poincaré's intuitions but only when using infinitesimal movement amplitudes. Such a limitation, originating from the use of standard linear mathematical tools, does not allow any experimental validation of the approach. Bootstrapping methods have been proposed to solve this problem [6]. For instance, Laflaquière et al. succeeded in extending the approach to much more realistic movement amplitudes by coupling a motor bootstrap technique with a Curvilinear Component Analysis (CCA) [7]. But all these approaches were criticized by Frolov in [8], claiming that they require a stable external environment during the exploration. Indeed, these works postulate some *a priori* knowledge of the environment that cannot be obtained by the sensory system only. As a solution, Frolov introduced a body endowed with tactile sensors and a mobile arm. While proprioceptive signals still encode the arm movements, the arm end-effector has to touch the body itself so as to ensure a stable perception, thus obtained without any prior hypothesis on the environmental state. Using a different approach, Laflaquière et al. have shown that, beyond the dimension of space, it is also possible to obtain an external space representation by using appropriate partitions of the motor space [9], resulting in a much more *motor oriented* than *sensor oriented* framework. In this contribution, each end-effector position of an arm is represented by the subset of the motor configurations leaving the sensory state invariant, the so-called *kernel manifolds*. But the limitations pointed out by Frolov apply here again, as a stable environmental state is still required.

This paper is focused on the extension of Laflaquière & al.'s approach to the building of an internal representation of an agent body, in the vein of Frolov's previous work. As outlined by Gapenne [10], body representation is of great importance in the understanding of the proprio-exteroception coupling, especially when facing the distal perception problem i.e. perceiving objects in space outside of the body. The goal is to prove, at first in a formal way, and then by means of computer simulations, that the sensorimotor representation of space proposed by Laflaquière & al can be extended to build an internal representation of the interaction between an agent with its own body. Recently, we have proposed a sketch of this work [11]. However the mathematical proof was inadequate and the simulations were limited to a very specific case. In this paper, an extension of [11] is proposed as more complete

solution to the body perception problem by using sensorimotor concepts. The internal kernel representation of the external space used in [9], [11], which is limited in this case to the body shape, is precisely mathematically formalized with proofs relying on the isomorphism theorems. Moreover a proof of the continuity of the internal representation is proposed, which is coherent with the external space continuity. This result is highlighted by the existence of a homeomorphic relation between the internal representation and the body space. As a result, it is shown that it becomes possible to build new motor commands by making interpolations in the internal kernel space. In other words, the internal representation can be successfully used to plan new movements of the body arm, i.e. movements built from motor configurations that have never been used before to obtain the internal representation. Motion planing is a well known robotics field that has been addressed by many researchers [12]–[14]. But the focus here is more to show the effectiveness of the internal sensorimotor representation rather than to propose another solution to path planning problems. In order to validate the approach in an efficient way, two kinds of experimentation are proposed, one using an agent endowed with an end-effector made of one finger, and the other with an end-effector made of two rigidly linked fingers. In both cases, two body shapes are considered, spherical and cubic, allowing a more general conclusion.

The paper is organized as follows. §II is devoted to the mathematical foundations of the proposed approach. Next, §III presents the simulated agents and the building of the internal representation in every considered cases. The results about internal representation are compared and discussed at the end of the section. The last section §IV is devoted to the motion planning problem using the sensorimotor representation. Obtained results with both spherical and cubic agents are presented and discussed. Finally, a conclusion ends the paper.

II. Towards a mathematical formalization

As a first step, this section is devoted to the formalization of the mathematical foundations required for building an internal representation of an agent's sensorimotor invariants. The first subsection is devoted to the formalization of the influence of the sensor pose on the consecutive sensations. Quotient sets will be introduced to mathematically describe the notion of sensory invariance, by regrouping all the sensor poses leading to the same sensation. In a second subsection, the agent body is introduced as a way to actively modify the sensor pose via its motor commands. This will allow to regroup, in a motor quotient set, all the motor commands leading to the same sensation, thus defining sensorimotor invariants. Their mathematical properties will be demonstrated, and exploited in Section III. A small discussion ends this section.

A. Sensory inputs and quotient set

Let's first consider a sensor (or a group of sensors), whose position and orientation in space is entirely captured by its pose $\mathbf{X} \in \chi$, with χ the *pose space*. χ is included inside the Special Euclidean group $SE(3)$, which is defined as the semidirect (noncommutative) product $SO(3) \ltimes \mathbb{R}^3$ with $SO(3)$

the 3D rotation group and $\mathbb{R}^3$ the 3D translation group. Indeed, the sensor pose is defined by a composition of one translation (the sensor position) and one rotation (the sensor orientation). For now, the sensor is considered *alone*: it is not connected to any agent body, which will be introduced in the next subsection. This sensor generates a sensation vector $\mathbf{S} = (s_1, s_2, \ldots, s_S)^T \in \mathcal{S}$, with $\mathcal{S} \subset \mathbb{R}^S$ the *sensory space*, and $.^T$ the transpose operator. Such a vector could originate from any modality, and/or could be the result of the concatenation of multiple sensor outputs; in such a case, it is supposed that these sensors are all rigidly stuck together. Importantly, by further restricting $\mathcal{S}$ to $\Sigma = \text{Im}(\phi_\epsilon)$, ϕ_ϵ can be rendered surjective from χ to Σ. In other words, Σ is the set of all "physically" reachable sensory states, and will thus also be called the *sensory space*. Note that ϕ_ϵ is not necessarily hypothesized as being a continuous function, and is considered non-injective, i.e. two different poses $\mathbf{X}_1$ and $\mathbf{X}_2$ can generate the same sensation $\mathbf{S}$. Such a property allows then to define an equivalence relation $=_{\phi_\epsilon}$ between any pair of pose $(\mathbf{X}_1, \mathbf{X}_2)$ of χ, such that

$$\mathbf{X}_1 =_{\phi_\epsilon} \mathbf{X}_2 \Leftrightarrow \exists \mathbf{S} \in \Sigma, \phi_\epsilon(\mathbf{X}_1) = \phi_\epsilon(\mathbf{X}_2) = \mathbf{S}. \quad (1)$$

It follows that $=_{\phi_\epsilon}$ is by definition the equivalence kernel of ϕ_ϵ. For any $\mathbf{X} \in \chi$ such that $\phi_\epsilon(\mathbf{X}) = \mathbf{S}$, let's now denote by $K_\mathbf{X}$ the equivalence class of $\mathbf{X}$, with

$$K_\mathbf{X} = \{\mathbf{R} \in \chi \mid \mathbf{R} =_{\phi_\epsilon} \mathbf{X}\}. \quad (2)$$

$K_\mathbf{X}$ can then be modded out to form the quotient set $\chi/_{=_{\phi_\epsilon}}$, with

$$\chi/_{=_{\phi_\epsilon}} = \{K_\mathbf{X} \mid \mathbf{X} \in \chi\}. \quad (3)$$

Then, one can denote π_{ϕ_ϵ} the quotient map from χ to its quotient set $\chi/_{=_{\phi_\epsilon}}$, mapping each pose $\mathbf{X}$ to its equivalent class $K_\mathbf{X}$.

Proposition 1. There exists a bijective function between the sets $\chi/_{=_{\phi_\epsilon}}$ and Σ.

Proof. Proposition 1 is trivial. The quotient set $\chi/_{=_{\phi_\epsilon}}$ is isomorphic (in the set-theory sense of a bijection) to its image Σ by ϕ_ϵ. Specifically, each equivalence class $K_\mathbf{X}$ corresponds to a unique sensation S. $\quad\square$

Figure 1 highlights the relationships between χ, Σ and $\chi/_{=_{\phi_\epsilon}}$. Regrouping all the sensor poses leading to the same sensation $\mathbf{S}$ in the same set $K_\mathbf{X}$ defines a so-called *pose kernel manifold* (gray area in χ). Each kernel manifold can then be conceptually represented in $\chi/_{=_{\phi_\epsilon}}$ by a point. Thanks to the equivalence relation $=_{\phi_\epsilon}$ (dotted line), each of them is also linked to a unique sensation $\mathbf{S}$ (green arrows). Indeed, since the forward sensory function ϕ_ϵ is surjective, then Proposition 1 also tells that there exists a bijective function between $\chi/_{=_{\phi_\epsilon}}$ and Σ. However $\chi/_{=_{\phi_\epsilon}}$ can only be built by regrouping all the sensor poses leading to the same sensation, while the agent does not have any way to actually *modify* them. To be exact, no agent has ever been considered so far. So lets now introduce the agent and its action capabilities in the formalism.
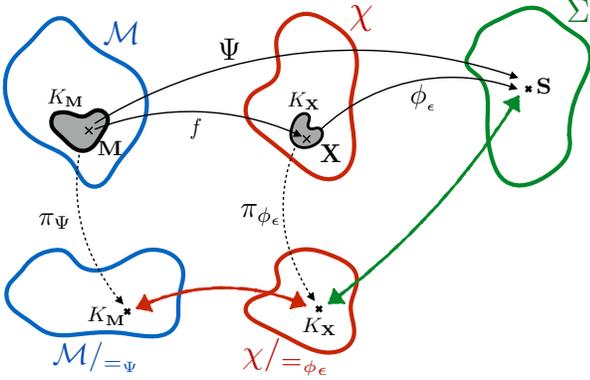
Fig. 1. Schematic representation of the different spaces involved in the paper. $\mathcal{M}$ is the motor space, χ is the pose space, Σ is the sensory space, $\mathcal{M}/_{=_\Psi}$ and $\chi/_{=_{\phi_\epsilon}}$ both represent the quotient sets the agent will actually build and represent, respectively.

B. Agent body and motor quotient set

Lets now consider a robotic system whose kinematics is inspired by traditional industrial robots. It is composed of moving rigid parts, each of them being connected to each other via a revolute joint parameterized by a scalar $m_i \in \mathbb{R}$, $i = \{1, \ldots, M\}$, see Fig. 2. The motor configuration of the agent is entirely described by the vector $\mathbf{M} = (m_1, m_2, \ldots, m_M)^T \in \mathcal{M}$, with $\mathcal{M} \in \mathbb{R}^M$ the so-called *motor configuration space*. One can assume without any loss of generality that the motor configuration space $\mathcal{M}$ is a compact M-dimensional manifold. The sensor previously mentioned in §II-A is now supposed rigidly linked to the end-effector of the system. Then, the sensor pose $\mathbf{X}$ will depend on the motor configuration $\mathbf{M}$. Using the forward kinematics model of the system $f(.)$, $\mathbf{X}$ can be computed from the motor configuration $\mathbf{M}$, i.e. $\mathbf{X} = f(\mathbf{M})$. Due to the possibility of redundancy, f can be surjective, as different motor configurations can lead to the same sensor pose. The f function also has the property of being a continuous, smooth, mapping from the compact manifold $\mathcal{M}$ to the pose space χ which is supposed Hausdorff. By extension, the quotient set $\chi/_{=_{\phi_\epsilon}}$ will also be hypothesized as Hausdorff.
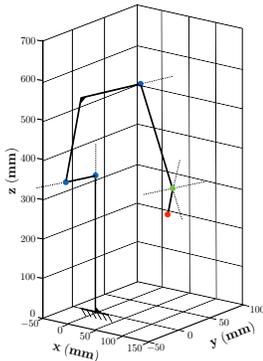

Fig. 2. Proposed robotic system. It is made of $M = 6$ degrees of freedom, each of them being controlled via a motor command m_i, $i = \{1, \ldots, M\}$ and moving the end-effector in the $3D$ space. Blue dots represent revolute joints, green dot depicts spherical joint, and the red dot indicates the end-effector.

As illustrated in Figure 1, a motor configuration $\mathbf{M}$ can now be associated to a sensation $\mathbf{S}$ thanks to the sensorimotor function $\Psi = \phi_\epsilon \circ f$. On this basis, and with the same reasoning as in §II-A, an equivalence relation $=_\Psi$ can be defined between any pair of vectors $(\mathbf{M}_1, \mathbf{M}_2)$ of $\mathcal{M}$, such that

$$\mathbf{M}_1 =_\Psi \mathbf{M}_2 \Leftrightarrow \exists \mathbf{S} \in \Sigma, \Psi(\mathbf{M}_1) = \Psi(\mathbf{M}_2) = \mathbf{S}. \quad (4)$$

Lets now denote $K_\mathbf{M}$ the equivalent class of $\mathbf{M}$, i.e.

$$K_\mathbf{M} = \{\mathbf{Q} \in \mathcal{M} \mid \mathbf{Q} =_\Psi \mathbf{M}\},$$
$$= f^{-1}(K_\mathbf{X}), \text{ with } \mathbf{X} \text{ such that } \phi_\epsilon(\mathbf{X}) = \mathbf{S}, \quad (5)$$

which can then be modded out to form the quotient set $\mathcal{M}/_{=_\Psi}$

$$\mathcal{M}/_{=_\Psi} = \{K_\mathbf{M} \mid \mathbf{M} \in \mathcal{M}\}. \quad (6)$$

Proposition 2. $\mathcal{M}/_{=_\Psi}$ is homeomorphic to $\chi/_{=_{\phi_\epsilon}}$.

Demonstration of Proposition 2 is written in Appendix A. Considering Proposition 1 and 2 together, one can then conclude that if the agent is able to build the quotient set $\mathcal{M}/_{=_\Psi}$ by regrouping all the motor commands leading to the same sensations $\mathbf{S} \in \Sigma$, then this quotient can be used by the agent to represent the quotient set $\chi/_{=_{\phi_\epsilon}}$. In other terms, the space of all reachable end-effector poses leading to a sensation $\mathbf{S} \in \Sigma$ is accessible to the agent by exploration of its sensorimotor invariants. The way the quotient set $\mathcal{M}/_{=_\Psi}$ is actually discovered and used in practice by the agent is illustrated in section III.

C. Interpretation and discussion

Proposition 2 hides, in some sense, the influence of the environment. Indeed, the existence of the quotient set $\mathcal{M}/_{=_\Psi}$ will be relevant to the agent only *for a fixed environmental state* ϵ during its exploration. This is clearly a strong *a priori* hypothesis faced by a lot of previous works [5], [6]. A first solution has been proposed in [8]: instead of independently analyzing proprio and exteroceptive data, the authors have proposed here to make them match together, with the idea that these two modalities must share common properties of space. This idea is illustrated with a simulated system made of a moving arm and a tactile body. With such a system, the approach allows the agent to build autonomously a 3D representation of space, which is obtained using a projection of proprioception and tactile data on a common representation, when the end effector touches the agent body. As a consequence, the environmental stationarity issue mentioned above does not hold anymore, the agent being in interaction only with its own body. Of course, the conclusions obtained with such an approach are thus limited to a representation of the body only, and do not capture any information about the space in which the agent is immersed. This paper is built on the same idea, and a tactile body will be introduced in the next section to allow the agent to build not only a representation of its own body, but also a topological image of the interaction with itself.

Another comment concerns the forward sensory function ϕ_ϵ, which is only supposed surjective thanks to the restriction of $\mathcal{S}$ to Σ (see §II-A). Such a property clearly allows one

to capture every case an agent might encounter during an exploration. Furthermore, regrouping all the sensor poses leading to the same sensation allows one to discard the possible system redundancy, and to build the quotient set $\chi/_{=_{\phi_\epsilon}}$ of the pose space χ through sensory invariants considerations. While possibly targeting the same kind of applications, "active approaches" to perception often explicitly model the structure of such a latent space. For instance, this allows the exploitation of independent variables, whose values can be modified by predefined control laws, in order to drive the system to an a priori targeted perception. The proposed sensorimotor approach allows instead the agent to autonomously build its so-called *internal representation* $\mathcal{M}/_{=_\Psi}$ by motor exploration and sensory invariants considerations without any a priori. So let's now focus on the way Proposition 2 can be exploited by an artifical agent to actually build $\mathcal{M}/_{=_\Psi}$.

III. BUILDING OF THE SENSORIMOTOR INTERNAL REPRESENTATION OF SIMULATED AGENT

It has been demonstrated that the quotient set $\mathcal{M}/_{=_\Psi}$ can be used as an internal representation of the quotient set $\chi/_{=_{\phi_\epsilon}}$. A simulated robotic system is now introduced in the following to illustrate (i) how $\mathcal{M}/_{=_\Psi}$ can actually be built from the sensorimotor flow of the simulated agent, and (ii) how $\mathcal{M}/_{=_\Psi}$ can then be used as an equivalent representation of $\chi/_{=_{\phi_\epsilon}}$ by the agent. This representation is then exploited for motion planning applications in Section IV. The description of the proposed simulated agent is proposed in a first subsection. The link between the mathematical considerations from §II and the proposed system will be carefully discussed in there. Then, the simulation setup and the algorithm for the building of $\mathcal{M}/_{=_\Psi}$ by the agent is provided in a second subsection. Finally, simulation results are provided in the last subsection.

A. Simulation setup and algorithm

1) Description of the proposed agent setup: In the following, the agent is made of a fixed spherical body covered with S tactile receptive fields and a multi-DoF arm similar to the one illustrated in §II, see Fig. 2. Note that a cubic body will also be introduced in §III-C1 to evaluate the genericity of the approach. The arm basis and the spherical body are affixed, so that only the arm is able to move thanks to its $M = 6$ actuators. In order to illustrate the genericity of the approach, 2 different arm end-effectors will be considered. In a first case, the end-effector is made of a single fingertip, i.e. a pointwise tool (see Figure 3-left). In a second case, a double fingertip –made of two distinct pointwise fingertips rigidly linked together– is used (see Figure 3-right). Whatever the end-effector, the sensation vector $\mathbf{S}$ will originate from the body endowed with a tactile modality, and not from a sensor placed at the end-effector configuration, as hypothesized in §II-B. But the tactile sensation will be supposed different from $\mathbf{0}$ only when the end-effector is in contact with the body (see Eq.(7) and (8)): in such a case, the origin of the sensation is not relevant anymore, and the formalization proposed in Section II still applies. Of course, the pose space χ will be now restricted to the end-effector pose $\mathbf{X}$, under the constraint
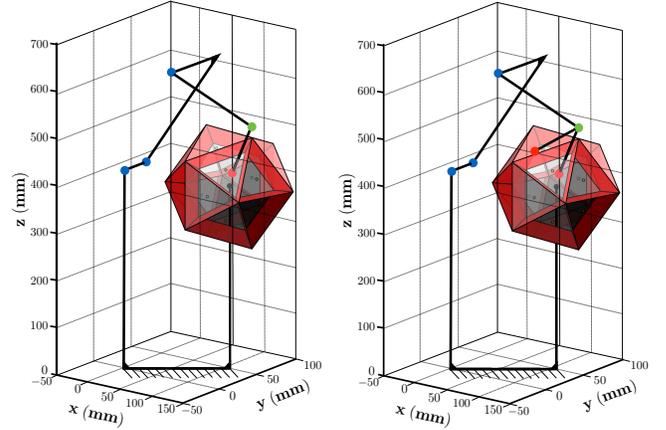

Fig. 3. Agent setup. (Left) The arm touches the spherical body endowed with S tactile receptive fields with a single fingertip tool. (Right) The arm is now endowed a double fingertip tool.

of the existence of a contact with the agent body. In other terms, depending on the nature of the contact with the body, the quotient set $\chi/_{=_{\phi_\epsilon}}$ will be different:

- *with only one pointwise contact with the body* (the *one* fingertip arm): in this case, the fingertip orientation will not have any influence on the corresponding tactile sensation generated by the body. Consequently, the quotient set $\chi/_{=_{\phi_\epsilon}}$, regrouping all the fingertip poses leading to the same sensation, will be entirely described by 2 latent variables, and can then be directly exploited to represent the 2-sphere body manifold inside a 3D euclidean space;
- *with two rigidly linked simultaneous pointwise contacts* (the *two* fingertips case): the fingertip pose will be now entirely described by three parameters: a position on the 2-sphere body and one orientation along the axis joining the two contact points.

Let's now precisely explain how the sensation $\mathbf{S}$ is actually obtained from the tactile agent body.

2) Sensation generation: Whatever the considered agent (with one or two fingertips), it is hypothesized that a contact with the full end-effector is mandatory to generate a non-null sensation vector $\mathbf{S}$. For the single fingertip end-effector, lets denote $\mathbf{X} \in \mathbb{R}^3$ the 3D-coordinates of a point in the euclidean space with respect to the arm basis frame. The ith sensory vector component of $\mathbf{S}$ is then computed along

$$s_i = \phi_i(\mathbf{X}) = \begin{cases} 0, & \text{if } \mathbf{X} \text{ is not on the body,} \\ \exp\left(-K\dfrac{\|\mathbf{X} - \mathbf{C}_i\|_2}{d_{\text{body}}}\right) & \text{otherwise,} \end{cases} \quad (7)$$

with $i = 1, \ldots, S$. $\mathbf{C}_i$ denotes the center of the ith sensitive field, K is a normalization constant, and d_{body} represents the spherical body diameter, see Figure 4. For the double fingertip contact case, lets denote $\mathbf{X}_1$ the first fingertip 3D-coordinates and $\mathbf{X}_2$ the second fingertip 3D-coordinates. Then, the ith
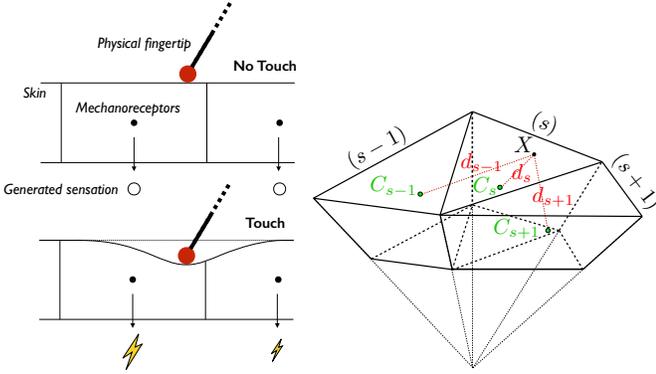
Fig. 4. Agent body tactile setup. (Left) The touch sensation is sparsely reproducing a simulated model of pressure sensors (mechanoreceptors) sensitive to a skin deformation. If the fingertip does not touch the skin, each mechanoreceptor sends a null signal, otherwise the value of the signal sent by each mechanoreceptor increases with the decrease of the distance to the fingertip. (Right) Surface of the body; each sensory vector component s_s depends on the distance between the contact point $\mathbf{X}$ and the sth sensitive field center $\mathbf{C}_s$, $s = 1, \ldots, S$. Note that the simulated receptive field depth is not infinitesimal, each has the same non-null thickness.

sensory vector component of $\mathbf{S}$ is computed along

$$s_i = \phi_i(\mathbf{X}) = \begin{cases} 0, \text{ if } \mathbf{X}_1 \text{ or } \mathbf{X}_2 \text{ is not on the body,} \\ \max_{k=1,2} \exp\left(-K\frac{\|\mathbf{X_k} - \mathbf{C}_i\|_2}{d_{\text{body}}}\right), \\ \qquad k = 1, 2 \qquad \text{otherwise.} \end{cases} \quad (8)$$

According to Eq. (8), only the smaller distance from each fingertip is considered. This constitutes a basic formalization of the masking effect originating from the bigger skin deformation. Note that Eq. (7) and (8) both define a surjective function ϕ from χ to Σ whose dependency to the environment has been discarded. Note also that, while being used to obtain the sensation vector $\mathbf{S}$ during the simulation, both equations are not known by the agent, which only has access to the resulting sensation $\mathbf{S}$.

B. Algorithm

This subsection is devoted to the description of the way the agent acquires, stores and processes its sensorimotor flow so as to build the quotient set $\mathcal{M}/_{=\Psi}$.

1) Rough random motor sampling: As already stated, it is supposed that the agent does not have access to its forward kinematics model $f(.)$. Consequently, the only naive operation it can conduct consists in randomly sampling its motor configuration space $\mathcal{M}$ by generating P random motor commands $\mathbf{M}[p] = (m_1[p], \ldots, m_M[p])^T$, each of them being next associated with a sensation $\mathbf{S}[p] = (s_1[p], \ldots, s_S[p])^T$, $p = 1, \ldots, P$. In all the following, a random walk model is applied to guide the agent motor space exploration, i.e.

$$m_i[p] = \mod (m_i[p-1] + \mu[p] + \pi, 2\pi) - \pi, i = 1, \ldots, M, \quad (9)$$

with $\mu[p]$ a realization of the random variable $\mu \sim \mathcal{N}(0, \sigma)$. A total of L trajectories, sampled with V values, are computed for each motor component, so that $P = L \times V$. Note that Eq. (9) is reset every V iterations to start a new random motor exploration (see the details in Algorithm 1).

2) Sensory vector generation: Each of the P motor configurations $\mathbf{M}[p]$ is associated to a sensor pose $\mathbf{X}[p] = f(\mathbf{M}[p])$ (recall that the agent does not have any access to it), together with a perception $\mathbf{S}[p]$ along $\mathbf{S}[p] = \Psi(\mathbf{M}[p])$. Of course, only a subset of the P sensation vectors are different from $\mathbf{0}$. This means that only a subset of the P motor commands has led to an arm end-effector in contact with the agent body. Additionally, multiple motor configurations can be related to the same non-null sensory vector because of the agent redundancy. But the random motor configuration sampling prevents the agent from *exactly* obtaining these sets of motor commands without any *a priori*. Consequently, *very close* sensations will be regrouped together up to a certain threshold, so as to estimate the motor quotient set. Let's now select N so-called *target sensations* $\mathbf{S}^{(i)}$, $i = 1, \ldots, N$ among all the R non-zero vectors $\mathbf{S}^*[r] \in \{\mathbf{S}[1], \ldots, \mathbf{S}[P]\} \subset \Sigma$, $r = 1, \ldots, R$. The N most distant vectors from each others are selected here in order to efficiently represent the sensory space Σ^*, see Algorithm 1 . One can then form the N sets $S^{(i)}$ regrouping all the $\mathbf{S}^{(i)}$ neighbors

$$S^{(i)} = \left\{ \mathbf{S}^*[r], r = 1, \ldots, R \mid d(\mathbf{S}^*[r], \mathbf{S}^{(i)}) < \delta/2 \right\}, \quad (10)$$

with $d(.)$ the Euclidean distance between two vectors and δ a threshold. Importantly, δ must be selected so as to avoid any intersection between all $S^{(i)}$, i.e.

$$\delta \leq \min_{i,j \in [1,N]^2} d(\mathbf{S}^{(i)}, \mathbf{S}^{(j)}). \quad (11)$$

3) Kernel space sampling: On this basis, one can then also form the N kernel sets $K_{\mathbf{M}}^{(i)}$ regrouping all the motor commands leading to a sensory vector in $S^{(i)}$, with

$$K_{\mathbf{M}}^{(i)} = \{\mathbf{M}^*[r], r = 1, \ldots, R \mid \mathbf{S}^*[r] = \Psi(\mathbf{M}^*[r]) \in S_i\}. \quad (12)$$

In other terms, $K_{\mathbf{M}}^{(i)}$ gathers all the motor commands $\mathbf{M}^*[r]$ such that the consequent sensor pose $\mathbf{X}[r]$ leads to a non-null perception vector $\mathbf{S}^*[r]$ in the set $S^{(i)}$. $K_{\mathbf{M}}^{(i)}$ then permits the definition of an approximation $\widehat{\mathcal{M}}/_{=\Psi}$ of the quotient set $\mathcal{M}/_{=\Psi}$ along

$$\widehat{\mathcal{M}}/_{=\Psi} = \left\{ K_{\mathbf{M}}^{(i)}, i = 1, \ldots, N \right\}. \quad (13)$$

4) Metric computations and low-dimensional projection: According to Proposition 2, $\mathcal{M}/_{=\Psi}$ contains topological information about $\chi/_{=\phi_\epsilon}$. It is expected that this property still applies for its discrete approximation $\widehat{\mathcal{M}}/_{=\Psi}$. Defining a metric on $\widehat{\mathcal{M}}/_{=\Psi}$ will indeed allow one to embed it in an Euclidean space where topological considerations can be observed. This can be achieved by considering a low dimensional projection of $\widehat{\mathcal{M}}/_{=\Psi}$, whose properties will depend on the nature of the contact with the agent body (see §III-A1). Importantly, note that from the agent point-of-view, such a low dimensional projection might not be mandatory. This projection is then only performed here to visualize and interpret the discrete quotient set $\widehat{\mathcal{M}}/_{=\Psi}$ built by the agent.

CCA (Curvilinear Component Analysis [15]) is used to perform such a projection. CCA is a non-linear projection technique which is used to represent, in a low dimensional

space, every point in $\widehat{\mathcal{M}}/_{=\Psi}$ by preserving the topology of the underlying manifold.

CCA is based on an iterative algorithm exploiting a self-organized neural network which minimizes a cost function assuring the conservation of the data topology through local distances preservation. In comparison with other well-known linear projection methods (PCA, or Metric Multidimensional Scalling [16]), CCA is able to deal with highly curved manifolds and gives better results in high-dimensional spaces than other non-linear methods [17]. Indeed, other non-linear dimension reduction algorithms, such as ISOMAP, Locally-Linear Embedding (LLE) and Laplacian Eigenmaps, have been tested on the data, but CCA empirically shows here the best projection results.

This projection is achieved by defining a metric in $\widehat{\mathcal{M}}/_{=\Psi}$ to actually obtain its low-dimensional representation. Let's first envisage $\widehat{\mathcal{M}}/_{=\Psi}$ as being a graph G with N nodes defined as the kernel sets $K_{\mathbf{M}}^{(i)}$, $i = \{1, \ldots, N\}$. Each node is connected to each other through edges weighted by their distances ρ. Taking two nodes/kernel sets $K_{\mathbf{M}}^{(i)}$ and $K_{\mathbf{M}}^{(j)}$ in G, one can then define the (pseudo)-distance $\rho(K_{\mathbf{M}}^{(i)}, K_{\mathbf{M}}^{(j)})$ along

$$\rho(K_{\mathbf{M}}^{(i)}, K_{\mathbf{M}}^{(j)}) = \min_{\substack{\mathbf{M}^*[r] \in K_{\mathbf{M}}^{(i)} \\ \mathbf{M}^*[s] \in K_{\mathbf{M}}^{(j)}}} d(\mathbf{M}^*[r], \mathbf{M}^*[s]). \quad (14)$$

This definition does not allow ρ to be a proper distance as the triangle inequality does not hold. Nevertheless, ρ can be slightly modified so as to define a proper distance between kernel sets. For instance, the Dijkstra's algorithm [18] can be exploited to find the shortest path between graph nodes. One then have a new metric $\tilde{\rho}$ defined as

$$\tilde{\rho}(K_{\mathbf{M}}^{(i)}, K_{\mathbf{M}}^{(j)}) = \text{path\_length}\big(\text{dijkstra}(G, K_{\mathbf{M}}^{(i)}, K_{\mathbf{M}}^{(j)})\big), \quad (15)$$

where path_length() return the sum of distances between two consecutive nodes in the shortest path returned by dijkstra().

In all the following, $\tilde{\rho}$ is used as the input space metric by CCA to obtain a low-dimensional representation of $\chi/_{=\phi_\epsilon}$. Importantly, the *a priori* knowledge of the output space dimension is not mandatory, as CCA itself can be used to estimate the intrinsic dimension of the input space to be projected. Such an application has already been proposed in [7] by the authors, and will not be addressed in this paper. Finally, Algorithm 1 summarizes all the previous steps, while their actual implementation is precisely depicted in the provided additional material.

C. Simulations and results

Let's now apply Algorithm 1 to the two agents quickly depicted in §III-A1. As already outlined, it will lead to two very different representations of the quotient set $\chi/_{=\phi_\epsilon}$ through the building of $\widehat{\mathcal{M}}/_{=\Psi}$.

1) First case: single fingertip agent: In such a case, the tactile sensation $\mathbf{S}$ only depends on the $3D$ position of the agent's fingertip on the body, since its orientation does not have any influence on $\mathbf{S}$. Then, $\chi/_{=\phi_\epsilon}$ can be seen as the image of the body $3D$ shape. This is illustrated in the two

---

Algorithm 1 Computation of the χ low-dim. representation

1: {Step 1: rough random motor sampling}
2: **for** each of the L motor trajectories **do**
3:    **for** each of the V motor configurations in the trajectory **do**
4:       Starting from an initial random motor configuration, perform a random walk, along Eq. (9),
5:       Collect the corresponding sensation if it is $\neq 0$.
6:    **end for**
7: **end for**
8:
9: {Step 2: kernel set sampling}
10: Pick N target sensations as uniformly as possible among those collected during step 1.
11: **for** each of the N target sensations **do**
12:    Cluster the sensations from step 1 that are the closest to the current target sensation, along Eq. (10),
13:    Append the motor configurations linked to these closest sensations in the corresponding motor kernel set, along Eq. (12).
14: **end for**
15:
16: {Step 3: computation of the metric}
17: Compute the distance between the kernel sets along Eq. (15).
18:
19: {Step 4 (optional): computation of a low-dim. projection through CCA}

---

next paragraphs, for two different body shapes (spherical and cubic).

a) Spherical body: In this first scenario, the agent body is made of $S = 20$ tactile receptive fields, thus forming an icosahedral body with a diameter $d_{\text{body}} = 100$mm. The normalization constant in Eq. (7) has been set to $K = 20$. The body center is placed at position $C = [30, 50, 100]$mm (to avoid any effect of symmetrization) in the frame $B_0 = (O_0, x_0, y_0, z_0)$ centered at the root basis of the robotic arm. The rough motor sampling step is performed with $L = 100$ trajectories of length $V = 10^6$ samples with a standard deviation parameter $\sigma = 0.1$, while $N = 1000$ target sensations $\mathbf{S}^{(i)}$ distant from a minimal euclidean distance of $\delta = 40.10^{-3}$ are selected. With all these parameters, Algorithm 1 is run with a final CCA projection performed in a $3D$ space. Such a low dimensional representation is indeed expected to be sufficient for representing the body topology. Nevertheless, any other larger dimension could be used without any other consequences on the conclusion than the difficulty to interpret the resulting projection. Then, the CCA output should provide a continuously deformed image of the original body shape, thanks to the homeomorphism property between $\mathcal{M}/_{=\Psi}$ and $\chi/_{=\phi_\epsilon}$ (see Proposition 2). But since $\mathcal{M}/_{=\Psi}$ is only approximated, it will be supposed that this property still holds with $\widehat{\mathcal{M}}/_{=\Psi}$. Additionally, an isometric transformation is applied to the $3D$ CCA output so as to represent this projection in the euclidean frame $B_0 = (O_0, x_0, y_0, z_0)$ of the agent, with a correct orientation and size. This will allow a direct comparison between the N target fingertip positions $\mathbf{X}^{(i)}$ such that $\phi(\mathbf{X}^{(i)}) = \mathbf{S}^{(i)}$, with the N isometrically-transformed CCA outputs. In practice, the isometric transformation relies on the Horn's quaternion-based method [19], which aims at minimizing the least square error between the target fingertip positions and the transformed CCA outputs.

Figure 5 (top) exhibits the simulation results. Subfigure 5(a) exhibits the ground-truth icosahedral agent body shape together with an artificial shading that has been added to
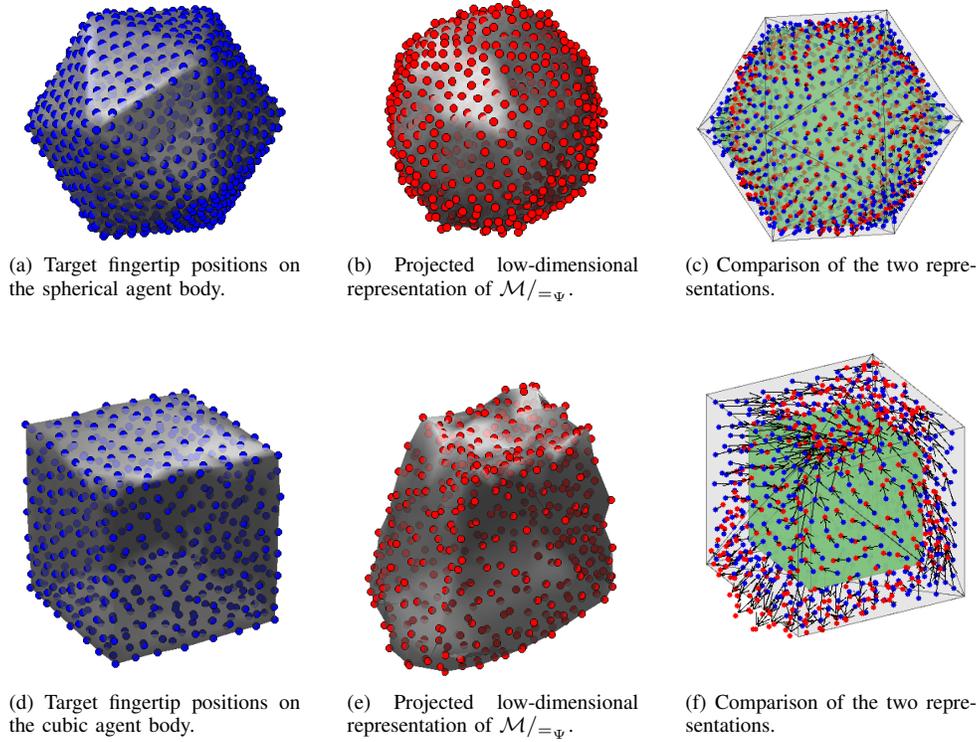
(a) Target fingertip positions on the spherical agent body.

(b) Projected low-dimensional representation of $\mathcal{M}/_{=_\Psi}$.

(c) Comparison of the two representations.

(d) Target fingertip positions on the cubic agent body.

(e) Projected low-dimensional representation of $\mathcal{M}/_{=_\Psi}$.

(f) Comparison of the two representations.

Fig. 5. Illustration of the agent internal representation for the N target sensations in the robotic $3D$ frame. (Red) isometrically-transformed internal representation of N target sensations by the agent, (Blue) original end-effector points that led to the target sensations. From the left to the right: (a/d) shaded body shape with target sensations on the surface (b/e) shaded recovered body shape (continuously deformed) with represented target sensation along the surface (c/f) arrows between transformed internal representation and real positions of target sensations on the body with tactile body fields in light gray and inner contours in green.

enhance its spatial shape. In this subfigure, the blue points represent the N target end-effector positions $\mathbf{X}^{(i)}$ on the body. Subfigure 5(b) represents the N transformed CCA outputs with red points. The added shading highlights a continuous deformation of the body original shape, but the extracted representation remains topologically similar to a sphere. Such a deformation might originate from (i) some projection errors by CCA, but also mainly from (ii) the distances between two motor configurations which is not maintained between the two subsequent end-effector poses. Indeed, since the forward kinematic model $f(.)$ is non-linear, $\mathcal{M}/_{=_\Psi}$ (and thus its approximation $\widehat{\mathcal{M}}/_{=_\Psi}$) is only homeomorphic to $\chi/_{=_{\phi_\epsilon}}$, and not isometric to it.

The blue and red points can be linked by pair as they both represent the same target fingertip position: one by its real position on the body (blue), and the other one by its (projected and isometrically transformed) internal representation (red). These links are represented by arrow in Subfigure 5(c) . Clearly, the two sets of points are consistent with each other, which means that the agent has been able to capture the body topology by using only sensorimotor information.

b) Cubic body: In order to illustrate the generality of the proposed approach, a second form of the agent body is used. This time, $S = 12$ tactile receptive fields (two by face) are used together to form a body with a cube shape of length $d_{\text{body}} = 100$mm. The normalization constant in Eq. (8) is now set to $K = 10$. The body center position, together with the

number of trajectories L, the samples number V and standard deviation σ remain unchanged, while δ has been now set to $\delta = 6.10^{-3}$. All the remaining steps in Algorithms 1 are the same, together with the CCA isometric transformation mentioned in the first simulation. The results are shown in the in Figure 5 (bottom), which again exhibits the target points on the body (blue) and those obtained by the construction of the internal representation (red). As already shown with the spherical body, it can be seen that the cubic shape has been deformed, for the same reason as those highlighted before, but is still recognizable. In other terms, the body topology has been correctly discovered by the agent.

2) Second case: double fingertips agent: Let's now consider the case of the agent endowed with an end-effector made of two rigidly linked fingers. As outlined in §III-A1, the quotient set $\chi/_{=_{\phi_\epsilon}}$ will be quite different from the one obtained in the previous subsection. Indeed, according to Eq. (8), a sensation $\mathbf{S}$ will be generated by the body only if the two fingertips simultaneously touch the body. Thus, all the fingertips poses generating the same sensation $\mathbf{S}$ are now entirely described by three independent parameters. This intuition is shown as correct in the following.

In this subsection, the agent's body is again made of the same spherical body than the one described in §III-C1, with a distance between the two fingertips set to $d_{\text{fingers}} = d_{\text{body}} = 100$mm. This time, Algorithm 1 is run with a final CCA projection performed in a 6D space. Consequently, the
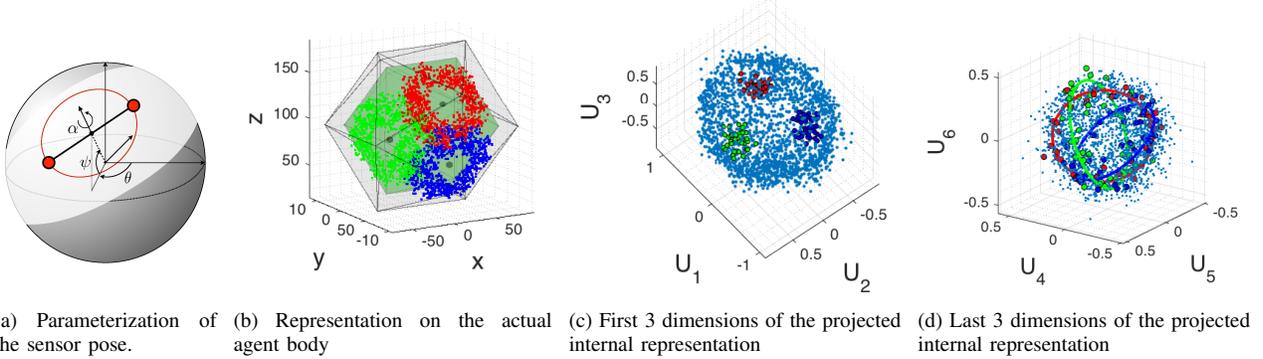
(a) Parameterization of the sensor pose.

(b) Representation on the actual agent body

(c) First 3 dimensions of the projected internal representation

(d) Last 3 dimensions of the projected internal representation

Fig. 6. (a) One possible parameterization of the double fingertips quotient space $\chi/_{=\phi_\epsilon}$, with $\psi \in [-\pi/2, \pi/2[$ the elevation, $\theta \in [0, \pi[$ the orientation of the middle-point between the two fingertips in spherical coordinates, and one parameter $\alpha \in [0, \pi[$ for the rotation along the radial axis. (b) After fixing three different middle-point positions on the spherical body, trace of fingertips positions (red, green and blue) along the rotation α with the average positions of its middle point in dark gray. (c) Representation in three chosen dimensions in the representation space of the middle point position. (d) Representation of the end-effector orientation α in the three remaining dimensions, with circles fitted to the points.

interpretation of such a projection will be far more complex than when working with a 3D projection like in the first case. The resulting projection and its corresponding interpretation is shown in Figure 6. As already outlined, the only poses of the end-effector in $SE(3)$ which generate a sensation **S** are those where the two fingertips are in contact with the body spherical surface. Such a constraint gives rise to a first interpretation of the quotient set $\chi/_{=\phi}$ as being the space of latent variables that describes all the possible configurations of two points distant by d_{fingers} on a sphere. This space then forms a manifold subset of $SE(3)$, which can be parameterized with a minimal number of 3 parameters, so that $\chi/_{=\phi_\epsilon}$ can be seen as a 3-manifold (manifold of intrinsic dimension equal to 3). One possible interpretation of these 3 parameters is proposed in Subfigure 6(a): two angles θ and ψ can be used to define the position of the middle-point between the two fingers, and one additional angle α captures the radial axis orientation of the two fingertips system. With such a parameterization, every pose of the two contact points, distant by d_{fingers} on the spherical body and leading to the same sensation **S**, can then be obtained.

Thanks to Algorithm 1, an internal (homeomorphic) representation $\widehat{\mathcal{M}}/_{=\Psi}$ of $\chi/_{=\phi_\epsilon}$ is obtained. Its corresponding 6D projection is shown in the two Subfigures 6(c) and (d), where the first 3 dimensions, followed by the 3 next ones are represented in two 3D points clouds plots. It is also shown in the same subfigures three different (arbitrary chosen) configurations in red, green and blue. Each color corresponds to fixed θ and ψ values, and to an α angle ranging from 0 to π. The corresponding configurations on the real agent body are also shown in Subfigure 6(b). Importantly, they do not exactly describe a circle on the spherical body because of the discrete approximation captured by Eq. (12). Subfigure 6(c) exhibits the first 3 dimensions of the projected internal representation. It is clear that these 3 first dimensions capture the middle point (joining the two fingertips) position on a sphere with a slightly smaller diameter than the spherical body. Indeed, close middle-points on the body correspond to close points in

this first 3D representation. One additional parameter needs to be considered to fully capture the internal representation. Indeed, the 3 next dimensions of the 6D projection of the internal representation, shown in Subfigure 6(d), exhibits the influence of the third parameter α, which draws circles on a 2-sphere. Here, each circle corresponds to a specific middle-point position in the first 3 dimensions, and uniting all of them then generates a sphere in the 3 last dimensions of the representation.

Again, all this effort to analyze and interpret the low-dimensional projection are only performed here to demonstrate that the quotient set $\mathcal{M}/_{=\Psi}$, and its approximation $\widehat{\mathcal{M}}/_{=\Psi}$, actually captures the topology of $\chi/_{=\phi_\epsilon}$. The agent does not need to perform such a projection to actually use the motor quotient set. This is illustrated in §IV with a motion planning application.

IV. MOTION PLANNING IN THE SENSORIMOTOR INTERNAL REPRESENTATION SPACE

The previous section was devoted to the building of a sensorimotor internal representation of the body agent. But why would the agent build such a map? From the authors point of view, this map is the first step towards the ability to plan a movement of the agent arm on the body. This section is mainly concerned with this kind of application, with the idea that one can infer the successive, never explored, motor commands to be applied so as to reach a given target sensation. This target sensation will be provided *a priori*, i.e. without any insight on an external goal, purpose or motivation of the agent. Such a problem is out of the scope of this paper and is a field of research on its own [20], [21]. From the mathematical proofs in §II, the continuity property of the homeomorphism between the motor and pose quotient sets is exploited to interpolate successive motor commands towards the sensor pose corresponding to the target sensation. The proposed algorithm allowing such an interpolation is described in a first subsection. On this basis, the two representations shown in §III-C2 are used in the second subsection to generate

successive, continuous motor orders from one initial sensor pose to the targeted one.

A. Motor interpolation algorithm

1) First step: towards a path in the motor quotient set $\mathcal{M}/_{=\Psi}$: The overall objective of the proposed sensorimotor motion planning approach is to find a motor strategy, which will allow the agent the reach a given target sensation through adequate, smooth, changes in the pose quotient set $\chi/_{=\phi_\epsilon}$. Thanks to Proposition 2, having smooth changes in $\chi/_{=\phi_\epsilon}$ is equivalent to smooth changes in $\mathcal{M}/_{=\Psi}$, i.e. in the internal representation of the agent. Such a property can be easily obtained by considering a step by step path in $\mathcal{M}/_{=\Psi}$, going from one kernel set $K_\mathbf{M} \in \mathcal{M}/_{=\Psi}$ to the next closest one. This way, having close kernel sets on the path in $\mathcal{M}/_{=\Psi}$ will conduct to small changes in $\chi/_{=\phi_\epsilon}$, and then to smooth changes of the pose of the sensor during the movement.

Recall that $\widehat{\mathcal{M}}/_{=\Psi}$ can be seen as a graph $G = (V, E)$, with $V = \{K_\mathbf{M}^{(i)}, i = 1, \ldots, N\}$ its nodes and E all its undirected edges (see §III-B4). Each edge between the ith and j^{th} node is weighted by the distance $d_{ij} = \rho(K_\mathbf{M}^{(i)}, K_\mathbf{M}^{(j)})$. Finding a path in $\widehat{\mathcal{M}}/_{=\Psi}$ is then analog to finding an optimal path in a graph, which is a very common task [22]. The following strategy is proposed:

(i) Compute a k-nearest neighbor graph $G_k = (V, E_k)$, where $E_k \subseteq E$ is composed of the k shortest edges of each nodes. k can be determined without *a priori* by optimization, see §IV-B.

(ii) In this graph G_k, compute the shortest path from node $K_\mathbf{M}^{(n)}$ to node $K_\mathbf{M}^{(m)}$ using Dijkstra algorithm. The resulting path P_{nm} is then an ordered length T list of successive kernel indexes (i), i.e.

$$P_{nm} = [n = p[1], p[2], ..., p[t], ..., p[T] = m]. \quad (16)$$

These two steps are illustrated in Figure 7. The quotient set $\mathcal{M}/_{=\Psi}$ is made of collection of motor kernel sets $K_\mathbf{M}^{(i)}$. Among them, a k-nearest neighbor graph G_k is computed, shown in gray in $\mathcal{M}/_{=\Psi}$. This graph connects a given motor kernel set $K_\mathbf{M}^{(i)}$ to its k closest neighbors according to the (pseudo-)distance ρ. From this graph, a path P is extracted (drawn in black), forming $K_\mathbf{M}^{(p[1])}$ to $K_\mathbf{M}^{(p[T])}$ (with $T = 4$ here).

2) Second step: trajectory in the motor space $\mathcal{M}$: Even if a path from the initial motor kernel set $K_\mathbf{M}^{(n)}$ to the final one $K_\mathbf{M}^{(m)}$ is defined in $\mathcal{M}/_{=\Psi}$, one still needs to determine the actual motor configuration $\mathbf{M}$ which must be used by the agent to move. A path must then be computed in the motor configuration space $\mathcal{M}$ *between* motor kernel sets, but also *inside* them. Such a problem is commonly referred to discrete motor planning in traditional mobile robotics, which is very common task [23]. Given the objective of minimizing *a priori* knowledge of the agent, a simple, straightforward and iterative interpolation strategy is proposed in this paper.

Lets consider two successive motor kernel sets $K_\mathbf{M}^{(p[t])}$ and $K_\mathbf{M}^{(p[t+1])}$ in the path P_{nm} obtained from Eq. (16), and an initial motor configuration $\mathbf{M}_1 \in K_\mathbf{M}^{(p[t])}$. The proposed algorithm follows these steps:
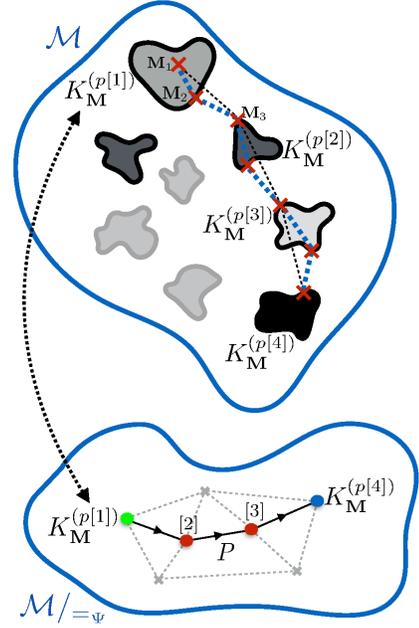

Fig. 7. Representation of the two step approach to plan a movement of length $T = 4$ from sensation $S^{(p[1])}$ to $S^{(p[4])}$. (i) The quotient set $\mathcal{M}/_{=\Psi}$ can be seen as a graph linking each kernel set it is made of. Using graph exploration algorithms allows one to define a path P in $\mathcal{M}/_{=\Psi}$ from the kernel sets $K_\mathbf{M}^{(p[1])}$ to $K_\mathbf{M}^{(p[4])}$. (ii) This path is then propagated in $\mathcal{M}$, where motor configuration interpolation is performed to move smoothly inside a kernel set, but also from one kernel to an other.

(i) determine the motor configuration $\mathbf{M}_3 \in K_\mathbf{M}^{(p[t+1])}$ such that

$$\mathbf{M}_3 = \arg \min_{\mathbf{M}^*[p] \in K_\mathbf{M}^{(p[t+1])}} d(\mathbf{M}^*[p], \mathbf{M}_1). \quad (17)$$

$\mathbf{M}_3$ is thus the closest motor configuration in the $t+1^{\text{th}}$ kernel set of the path P_{nm} to $\mathbf{M}_1$. But jumping from $\mathbf{M}_1$ to $\mathbf{M}_3$, i.e. directly from one motor kernel set to an other, is suboptimal w.r.t. to the interkernel distance. An additional, intermediate, motor configuration $\mathbf{M}_2$ is then computed.

(ii) determine the motor configuration $\mathbf{M}_2 \in K_\mathbf{M}^{(p[t])}$ such that

$$\mathbf{M}_2 = \arg \min_{\mathbf{M}^*[p] \in K_\mathbf{M}^{(p[t])}} d(\mathbf{M}^*[p], \mathbf{M}_3). \quad (18)$$

$\mathbf{M}_2$ thus defines an additional motor configuration in the tth motor kernel set of the path P_{nm}.

(iii) interpolate I intermediate motor configuration between $\mathbf{M}_1$ and $\mathbf{M}_2$, but also between $\mathbf{M}_2$ and $\mathbf{M}_3$ with any interpolation function $g(.)$ (in this paper, the `interp1` MATLAB function is used).

These three steps are then repeated from one motor kernel set to another inside the path P_{nm}. The implementation of this interpolation in $\mathcal{M}$ is summarized in Algorithm 2. A detailed version of this algorithm is also provided in the additional material; in addition to the three steps mentioned above, the detailed algorithm exhibits an optimization which is performed to find the trajectory minimizing the maximal inter-kernel distance, among all the trajectories starting from a random motor configuration in the initial motor kernel set.

This simple approach is illustrated in Figure 7. The motor configuration space $\mathcal{M}$ is made of multiple motor kernel sets $K_{\mathbf{M}}^{(i)}$. The path found according to §IV-A1 in the motor quotient set $\mathcal{M}/_{=\Psi}$ allows one to select successive motor kernel sets in $\mathcal{M}$, starting from $K_{\mathbf{M}}^{(t[1])}$ to the final one $K_{\mathbf{M}}^{(t[4])}$ in this illustration. Figure 7 also shows the three motor configurations $\mathbf{M}_1$, $\mathbf{M}_2$ and $\mathbf{M}_3$ determined for the two first kernel sets of P. The trajectory in $\mathcal{M}$ exhibits different kind of movement. The first movement, going from $\mathbf{M}_1$ to $\mathbf{M}_2$, is performed *inside* the motor kernel set $K_{\mathbf{M}}^{(p[t])}$. It then produces a movement of the arm letting invariant the fingertip pose in $\chi/_{=\phi_\epsilon}$. The second movement, going from $\mathbf{M}_2$ to $\mathbf{M}_3$, is made *between* the two motor kernel sets $K_{\mathbf{M}}^{(p[t])}$ and $K_{\mathbf{M}}^{(p[t+1])}$. An interpolation then defines successive intermediate motor configurations from one motor kernel set to another. As already outlined, given the homeomorphism property existing between $\mathcal{M}/_{=\Psi}$ and $\chi/_{=\phi_\epsilon}$, such successive close motor configurations are expected to correspond to successive close fingertip poses, i.e. the arm end-effector should smoothly go from one pose to another. This is verified in the next subsection.

Algorithm 2 Motor interpolation

1: {Step 1: path in the discrete quotient set $\widehat{\mathcal{M}}/_{=\Psi}$}
2: Compute a k-nearest neighbors graph G_k from graph $\widehat{\mathcal{M}}/_{=\Psi}$ using the $\tilde{\rho}$ pseudo-metric defined in Eq.(15).
3: Find the shortest path P in the graph G_k from the initial kernel set to the final one.
4:
5: {Step 2: trajectory in the motor configuration space $\mathcal{M}$}
6: Find iteratively the successive motor configurations $\mathbf{M}_1$, $\mathbf{M}_2$ and $\mathbf{M}_3$ in $\mathcal{M}$ using §IV-A2 to go from one kernel set to the next one in the path obtained from step 1.
7:
8: {Step 3: interpolation between motor configurations in $\mathcal{M}$}
9: Use interpolation between the motor configurations from step 2 to obtain the actual successive motor commands to be applied to the system.

B. Results

Algorithm 2 is run on the spherical and cubic body described in §III-C1. In each case, the graph G contains $N = 1000$ nodes, one for each motor kernel set $K_{\mathbf{M}}^{(i)}$ corresponding to 1000 target sensations $\mathbf{S}^{(i)}$, and almost $5 \cdot 10^5$ edges. The number of edges is quickly reduced by computing the k-nearest neighbors graph G_k. While the number k of neighbors can be given *a priori*, it can also be selected by running successive iterations of Algorithm 2 and finding the value producing the minimum maximal inter-kernels distance.

One then needs to define starting and ending target sensations; these are selected here so that the corresponding poses of the arm end-effector on the body are the farthest possible to each other. The starting and ending poses are shown by the green (start) and blue (end) poses respectively on Subfigure 8 (a) and (d) (more generally, the color conventions between Figure 8 and 7 are identical to ease the interpretation). The optimal number of neighbors k is found to be $k = 12$ and $k = 15$, leading to a path P of length $T = 7$ and $T = 6$, for the spherical and cubic body respectively. This path, while being computed directly in the discrete internal representation $\widehat{\mathcal{M}}/_{=\Psi}$, can also been visualized in its 6D

representation shown in the two Subfigures 6(c) and (d). The same representation is shown again in Subfigures 8(b) and (c), together with the motor path P drawn with black lines. In these two subfigures, nodes/motor kernel sets in P are shown as red circles, while the corresponding initial and final sets are again in green and blue respectively. As already outlined, the path P in $\widehat{\mathcal{M}}/_{=\Psi}$ must then be propagated in the actual motor configuration space $\mathcal{M}$ of the agent using the second step of Algorithm 2. The resulting successive motor configurations M_1, M_2 and M_3 (iteratively computed for each motor kernel set) lead to three poses X_1, X_2 and X_3 shown as red crosses in Subfigure 8 (a) and (d). Next, additional interpolated motor configurations are added in between, leading to the changes in the end-effector pose shown in blue dotted lines. As a result, a trajectory of the arm end-effector (i.e. the two fingertips), from the initial pose to the final one on the agent body, is extracted. Subfigure 8(a) also shows identical numbers $[i]$ on the trajectory. This number, which represents a lightweight notation for $K_{\mathbf{M}}^{(p[i])}$ indicates that the two concerned end-effector poses are obtained from the same motor kernel set (i.e. are obtained with a movement from $\mathbf{M}_1$ to $\mathbf{M}_2$ *inside* the same motor kernel set). These poses should then be theoretically identical, but the discrete approximation $\widehat{\mathcal{M}}/_{=\Psi}$ of $\mathcal{M}/_{=\Psi}$ prevents this. Nevertheless, it can be seen from these two trajectories computed for two different body geometries, that the end-effector stays smoothly inside the tactile fields of the body along the consequent trajectory. As expected, it moves almost straightly between motor kernel sets, even though the transitional end-effector poses are quite far from each other w.r.t. the body scale[1].

V. CONCLUSION

This paper studies the construction of a sensorimotor representation of a naive agent's tactile space. Before actually focusing on a specific modality, a careful generic mathematical formalization of the notion of "sensorimotor invariants" is proposed. Based on the properties of motor and sensor pose quotient sets, it demonstrates that an internal motor representation of all reachable sensor poses is accessible to the agent by exploration of its sensorimotor invariants. On this basis, a simulated robotic system, endowed with an arm and a body with tactile capabilities, is introduced so as to illustrate how such a representation can be actually built. An algorithm is then proposed to obtain a low-dimensional projection of it, allowing one to understand and interpret the resulting graph. Tested with two tactile body geometries, and two end-effector configurations, results show that the proposed approach can be exploited by the agent to obtain a sensorimotor image of its own body, with minimal *a priori* information. Then, as an illustrative application, this internal motor representation is used to generate motor commands. While based on a discrete approximation of the quotient sets, a second algorithm iteratively provides interpolated motor commands producing a smooth arm movement, as expected by the theory.

---

[1]Two video attachments have been uploaded together with this submission. They show the movement performed by the agent for the two cases in Subfigure 8 (a) and (d).
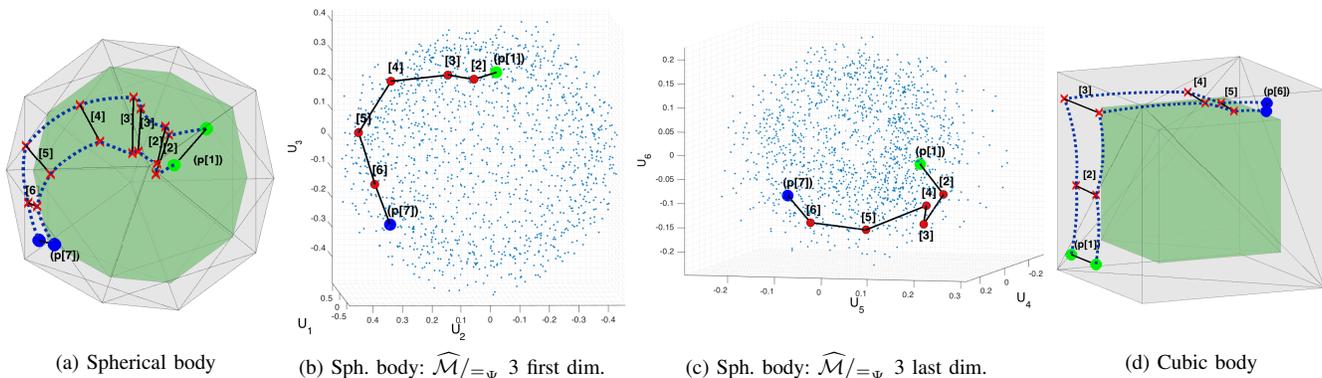
Fig. 8. Motion planning, performed with the agent endowed with two fingertips, and for a spherical or cubic body. The two trajectories on the actual agent body are shown in (a) and (d) for the two body geometries. The corresponding path in the discrete motor quotient set $\widehat{\mathcal{M}}/_{=_\Psi}$, where the interpolation is actually performed, is shown in (b) and (c) for the spherical body. The same color conventions as in Figure 7 are used.

The proposed formalism, while illustrated here with an agent endowed with tactile capabilities, is explicitly written in very generic terms. It can then be applied to other sensory modalities, like vision, as partially shown by the authors in [9]. Concerning the tactile modality, this paper is philosophically close to the approach by A.A. Frolov in [24]. But the proposed work goes far beyond the estimation of dimension like in [8], as an abstract representation emerges from the sole sensorimotor interaction of the agent with its own body. Furthermore, it can also be exploited by the agent to actually reach any target sensation. Importantly, the proposed formalism is rooted in purely sensorimotor considerations. Consequently, the obtained internal representation only appears thanks to the sensorimotor invariants of its own interaction, and can thus not be considered as an objective representation of the world, as outlined by K. O'Regan in [4].

From now on, can we finally say that the agent is actually "perceiving" the world? It is clear that the conclusions outlined in this paper are at best limited to the agent body. Even if the proposed framework is expected to be the first step towards a more complete mathematical formalization of the sensorimotor approach, one still needs to bridge the gap with the environment in which the agent is immersed. Extending the internal representation to capture invariant properties of the interaction between an agent and its environment will undoubtedly constitute a challenging task. However this is mandatory to bring out the more generic notion of "space perception", which will allow the agent to differentiate itself from the environment, and thus to elaborate the notion of distal perception.

APPENDIX A
PROOF OF PROP. 2: $\mathcal{M}/_{=_\Psi}$ IS HOMEOMORPHIC TO $\chi/_{=_{\phi_\epsilon}}$.

The following definitions and propositions are quite classical mathematical considerations [25], [26]. They are recalled for self-containedness.

Let X be a topological space endowed with the topology $\mathcal{T}$, $\sim$ be an equivalence relation, and $X/_\sim = \{x \in X | x \sim y, y \in X\}$ be the quotient space of X with respect to $\sim$. Let's denote $\pi : X \to X/_\sim$ the natural surjective map from each

point in X to its equivalent class. Then one can endow $X/_\sim$ with the *quotient topology* $\mathcal{T}_\pi$ by taking the open sets in $X/_\sim$ that are also open sets in X through π^{-1}, i.e.

$$\mathcal{T}_\pi = \{U \subseteq X | \pi^{-1}(U) \in \mathcal{T}\}.$$

This constitutes the finest topology on $X/_\sim$ such that π is continuous. This leads to the following propositions.

Proposition 3. Let X and Y be topological spaces. The surjective map $\hat{f} : X \to Y$ is called a *quotient map* if it has the property :

$$U \text{ is open in } Y \Leftrightarrow \hat{f}^{-1}(U) \text{ is open in } X.$$

Proposition 4. Let $\hat{f} : X \to Y$ be a continuous surjective map. If $\hat{f}$ is a closed map (takes closed sets in X to closed sets in Y) then $\hat{f}$ is a quotient map.

Proof. Let's show the property from proposition 3 :
$\Rightarrow$ Note U an open set in Y. $\hat{f}$ continuous implies that $\hat{f}^{-1}(U)$ is open in X.
$\Leftarrow$ Let's take U a subset of Y such that $\hat{f}^{-1}(U)$ is open in X. Thus the complement $\overline{\hat{f}^{-1}(U)} = X - \hat{f}^{-1}(U)$ is closed in X. $\hat{f}$ being a closed map, $\hat{f}(X - \hat{f}^{-1}(U)) = \hat{f}(\hat{f}^{-1}(Y) - \hat{f}^{-1}(U)) = \hat{f}(\hat{f}^{-1}(Y - U)) = Y - U = \overline{U}$ is closed. Thus U is open in Y.
Thus $\hat{f}$ is a quotient map. $\square$

Proposition 5. Let $\hat{f} : X \to Y$ be a continuous surjective map. If X is compact and Y is Hausdorff, then $\hat{f}$ is a quotient map.

Proof. Note C a closed set in X. Since X is compact, C is compact too. Thus $\hat{f}(C)$ is a compact subset of Y, and since Y is Hausdorff, $\hat{f}(C)$ is a closed set in Y. $\hat{f}$ is then a closed map, hence thanks to Proposition 4, $\hat{f}$ is a quotient map too. $\square$

Proposition 6. Let $\hat{f} : X \to Y$ a continuous surjective map and $=_{\hat{f}}$ the induced equivalence relation. Set

$$X/_{=_{\hat{f}}} = \{x \in X | \hat{f}(x) = y \in Y\}$$

the quotient space of X with respect to $\hat{f}$, let $\pi : X \to X/_{=\hat{f}}$ be the projection from any point $x \in X$ to its equivalent class $K_x = \{a \in X | a =_{\hat{f}} x\}$, and give $X/_{=\hat{f}}$ the quotient topology $\mathcal{T}_\pi$ defined above. If X is compact and Y is Hausdorff, then the function $h : X/_{=\hat{f}} \to Y$ defined as follows: for all $x \in X$, $h(\pi(x)) = \hat{f}(x)$, is a homeomorphism.

$$
\begin{array}{ccc}
X & \xrightarrow{\hat{f}} & Y \\
\pi \downarrow & \nearrow h & \\
X/_{=\hat{f}} & &
\end{array}
$$

Proof. To prove that h is a homeomorphism it is sufficient to show that (i) h and (ii) h^{-1} are continuous, and that (iii) h is a bijection.

(i) Let's show that h^{-1} is continuous: from Proposition 5, $\hat{f}$ is a quotient map. Let V be an open set in $X/_{=\hat{f}}$, $V \in \mathcal{T}_\pi$, and $\pi^{-1}(V) \in \mathcal{T}$, so it is an open set in X. Since $\pi^{-1}(V) = \hat{f}^{-1}(h(V))$, and since $\hat{f}$ is a quotient map, then $h(V)$ is open in Y. Thus $\hat{h}^{-1} : Y \to X/_{=\hat{f}}$ is continuous.

(ii) Let's show that h is continuous: note $U \subset Y$ an open set in Y. Since $\pi^{-1}(h^{-1}(U)) = \hat{f}^{-1}(U)$, and since $\hat{f}$ is continuous, then $\hat{f}^{-1}(U)$ is open. Consequently, $h^{-1}(U) \in \mathcal{T}_\pi$ is open too, so that h is continuous.

(iii) From the application of the first isomorphism theorem, one can directly say that h is a bijection.

Thus, h is a homeomorphism. $\qquad\square$

Applying Proposition 6 with $X = \mathcal{M}$ compact, $Y = \chi/_{=\phi_\epsilon}$ Hausdorff, and $\hat{f} = \pi_{\phi_\epsilon} \circ f$ a continuous surjective function by composition of two continuous surjective functions, leads to the proof that there exists a homeomorphism between $\mathcal{M}/_{=\hat{f}}$ and $\chi/_{=\phi_\epsilon}$. Since $\mathcal{M}/_{=\hat{f}} = \mathcal{M}/_{=\Psi}$ ($=_{\hat{f}}$ is equivalent to $=_\Psi$ thanks to the bijection between $\chi/_{=\phi_\epsilon}$ and Σ), then Proposition 2 follows.

REFERENCES

[1] H. Poincaré, "Paris: La science et lhypotheèse," *Flammarion*, 1902.

[2] ——, "Science and hypothesis," *London: Walter Scott Publishing*, 1905.

[3] ——, "L'espace Et la Géométrie," *Revue de Métaphysique Et de Morale*, vol. 3, no. 6, pp. 631–646, 1895.

[4] J. K. O'Regan and A. Noë, "A sensorimotor account of vision and visual consciousness." *The Behavioral and brain sciences*, vol. 24, no. 5, pp. 939–973; discussion 973–1031, Oct. 2001.

[5] D. Philipona, J. K. O'Regan, and J.-P. Nadal, "Is there something out there?: Inferring space from sensorimotor dependencies," *Neural Comput.*, vol. 15, no. 9, pp. 2029–2049, 2003.

[6] D. Philipona, J. K. O'Regan, J.-P. Nadal, and O. J.-M. Coenen, "Perception of the structure of the physical world using unknown sensors and effectors," *Advances in Neural Information Processing Systems*, vol. 15, 2004.

[7] A. Laflaquière, S. Argentieri, O. Breysse, S. Genet, and B. Gas, "A non-linear approach to space dimension perception by a naive agent," in *Intelligent Robots and Systems (IROS), 2012 IEEE/RSJ International Conference on*, 2012, pp. 3253–3259.

[8] V. Y. Roschin and A. Frolov, "A neural network model for the acquisition of a spatial body scheme through sensorimotor interaction," *Neural Computation*, vol. 23, pp. 1821–1834, 2011.

[9] A. Laflaquière, J. K. O'Regan, S. Argentieri, B. Gas, and A. Terekhov, "Learning agents spatial configuration from sensorimotor invariants," *Robotics and Autonomous Systems*, vol. 71, pp. 49–59, September 2015.

[10] O. Gapenne, "The co-constitution of the self and the world: action and proprioceptive coupling," *Frontiers in Psychology*, vol. 5, 2014.

[11] V. Marcel, B. Garcia, S. Argentieri, and B. Gas, "Building the representation of an agent body from its sensorimotor invariants," in *Workshop on Sensorimotor Contingencies for Robotics, IEEE/RSJ International Conference on Intelligent Robots and Systems, IROS'15*, 2015.

[12] E. Koditschek, "Exact robot navigation by means of potential functions: some topological considerations," *IEEE International Conference on Robotics and Automation*, pp. 1–6, 1987.

[13] T. Lozano-Perez, "Automatic planning of manipulator transfer movements," *IEEE Transactions on SMC*, vol. 11, no. 10, pp. 681–698, 1981.

[14] L. Jaulin, "Path planning using intervals and graphs," *Reliable Computing*, vol. 7, no. 1, pp. 1–15, 2001.

[15] P. Demartines and J. Herault, "Curvilinear component analysis: a self-organizing neural network for nonlinear mapping of data sets." *IEEE Transactions on Neural Networks*, vol. 8, no. 1, pp. 148–54, Jan. 1997.

[16] H. Abdi, "Metric multidimensional scaling," *Encyclopedia of Measurement and Statistics*, vol. 3, pp. 599–605, 2007.

[17] J. A. Lee and M. Verleysen, *Nonlinear Dimensionality Reduction*, 1st ed. Springer Publishing Company, Incorporated, 2007.

[18] E. W. Dijkstra, "A note on two problems in connexion with graphs," *Numerische Mathematik*, vol. 1, no. 1, pp. 269–271, 1959.

[19] B. K. P. Horn, "Closed-form solution of absolute orientation using unit quaternions," *Journal of the Optical Society of America A*, vol. 4, no. 4, pp. 629–642, 1987.

[20] P.-Y. Oudeyer, F. Kaplan, and V. Hafner, "Intrinsic motivation systems for autonomous mental development," *Evolutionary Computation, IEEE Transactions on*, vol. 11, no. 2, pp. 265–286, April 2007.

[21] A. Maye and A. K. Engel, "Extending sensorimotor contingency theory: prediction, planning, and action generation," *Adaptive Behavior*, vol. 14, pp. 1–14, aug 2013.

[22] J.-A. Bondy and U. S. R. Murty, *Graph theory*, ser. Graduate texts in mathematics. New York, London: Springer, 2007.

[23] S. M. LaValle, *Planning Algorithms*. New York, NY, USA: Cambridge University Press, 2006.

[24] A.A.Frolov, "Physiological basis of 3-D external space perception : approach of Henri Poincaré," in *History of the neurosciences in France and Russia*, hermann ed., 2011.

[25] K. Joshi, *Introduction to General Topology*. Wiley Eastern, 1983.

[26] N. Bourbaki, *General Topology*, ser. Actualités scientifiques et industrielles. ADDISON-WESLEY, 1966, no. ptie. 1.
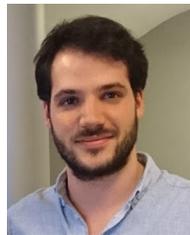
Valentin Marcel received the M.Sc degree in applied mathematics, in 2015 from the École Normale Supérieure, France. He is currently a Ph.D. fellow at the Institut des Systèmes Intelligents et de Robotique UMR 7222, Pierre et Marie Curie University, Paris, France. His research interests include developmental robotics, computational neuroscience especially to study the sensorimotor perception of space in robotics using tools such as topological data analysis and machine learning.

Sylvain Argentieri obtained the highest teaching diploma in France (Agrégation externe) in Electronical Science from the École Normale Superieure in 2002. He then received his Ph.D. in Computer Science from the Paul Sabatier University (Toulouse) in 2006. He is now Associate Professor with the "Interaction" group in the Institute for Intelligent Systems and Robotics (ISIR), Pierre et Marie Curie University, since 2008. His research interests relate to artificial perception in a robotics context –with a focus on auditory perception–, but also to active approaches to multimodal perception and sensorimotor integration.

Bruno Gas obtained his Ph.D. in Biologically Inspired Neural Networks at the Orsay University Paris 11 (1994). He became Associate professor in the ENSEA engineering school (1994), and then in the Instruments and Systems Laboratory at the Pierre et Marie Curie University (1997). He then obtained his habilitation in 2005, while he became the ISIR (Institute for Intelligent Systems and Robotics) SIMA (Mobile and Autonomous Integrated Systems) group leader in 2007. He is now full time professor since 2010 with the "Interaction" group in ISIR. His current research interests include self-organized neural networks, sensorimotor perception and robot hearing.